AD-A226 636

TATION PAGE

Form Approved
OMB No. 0704-0188

(2)

1. Agency Use Only (Leave blank).	2. Report Date.	3. Report Type and Dates Covered.
	1989	Journal Article

4. Title and Subtitle.
Applications and time-domain solution of higher-order parabolic equations in underwater acoustics

5. Funding Numbers.
Program Element No. 61153N
Project No. 3202
Task No. OH0
Accession No. DN257015

6. Author(s).
Michael D. Collins

7. Performing Organization Name(s) and Address(es).
Naval Oceanographic and Atmospheric Research Laboratory*
Stennis Space Center, MS 39529-5004

8. Performing Organization Report Number.
JA 221:021:89

9. Sponsoring/Monitoring Agency Name(s) and Address(es).
Naval Oceanographic and Atmospheric Research Laboratory*
Stennis Space Center, MS 39529-5004

10. Sponsoring/Monitoring Agency Report Number.
JA 221:021:89

11. Supplementary Notes.
*Formerly Naval Ocean Research and Development Activity

12a. Distribution/Availability Statement.
Approved for public release; distribution is unlimited.

12b. Distribution Code.

13. Abstract *(Maximum 200 words).*

A higher-order parabolic equation and the corresponding higher-order time-domain parabolic equation are derived from a Pade series and solved numerically. These models provide accurate solutions for problems involving very-wide-angle propagation (e.g., propagation in the nearfield or over a hard ocean bottom); propagation in domains in which sound-speed variations are large (e.g., propagation in deep water, deep within the ocean bottom, in high-speed ocean bottoms, and possible of different wave types); and propagation out to very long ranges. The possibility of modeling elastic wave propagation with a similar approach is considered.

14. Subject Terms.	15. Number of Pages.
(U) Transients; (U) Distributed Sensors; (U) Coherence; (U) Detection; (U) Classification	16. Price Code.

17. Security Classification of Report.	18. Security Classification of This Page.	19. Security Classification of Abstract.	20. Limitation of Abstract.
Unclassified	Unclassified	Unclassified	SAR

NSN 7540-01-280-5500

Standard Form 298 (Rev. 2-89)
Prescribed by ANSI Std. Z39-18
298-102

90 09 17 118

Applications and time-domain solution of higher-order parabolic equations in underwater acoustics

Michael D. Collins[a)]
Naval Ocean Research and Development Activity, Stennis Space Center, Mississippi 39529

(Received 9 February 1989; accepted for publication 19 May 1989)

A higher-order parabolic equation and the corresponding higher-order time-domain parabolic equation are derived from a Padé series and solved numerically. These models provide accurate solutions for problems involving very-wide-angle propagation (e.g., propagation in the nearfield or over a hard ocean bottom); propagation in domains in which sound-speed variations are large (e.g., propagation in deep water, deep within the ocean bottom, in high-speed ocean bottoms, and possibly of different wave types); and propagation out to very long ranges. The possibility of modeling elastic wave propagation with a similar approach is considered.

PACS numbers: 43.30.Bp, 43.20.Bi

INTRODUCTION

The parabolic equation (PE) has undergone extensive development since it was first applied to underwater acoustics[1] including improvements in accuracy and implementation in the time domain. The phase errors of PE solutions, which approximate the solution of the wave equation, were reduced significantly with the introduction of the wide-angle PE.[2-4] Although various generalizations of the wide-angle PE have been considered,[5-7] the aperture limitation of the PE has remained an issue of concern. The time-domain parabolic equation (TDPE)[8-12] allows one to perform pulse propagation calculations without Fourier synthesis. The TDPE has been extended to handle interface conditions,[9] nonlinear propagation,[10] density variations and sediment attenuation,[11] and wide-angle diffraction and sediment dispersion.[12]

In this article, a higher-order PE based on a Padé series[7] is shown to provide solutions comparable in accuracy to normal-mode solutions for problems involving very-wide-angle propagation, large variations in sound speed, and propagation out to long range. Since the Padé series is composed of rational linear terms, the higher-order PE is easy to solve numerically. The corresponding higher-order TDPE is solved numerically and compared with a wide-angle TDPE designed for propagation in shallow water.[12] The possibility of applying the Padé series to derive a PE for elastic wave propagation is investigated.

I. THE HIGHER-ORDER PE

A time-harmonic steady state is assumed, and the acoustic pressure p is factored as $p(\mathbf{x},t) = P(\mathbf{x})\exp(-i\omega t)$, where t is time, $\mathbf{x}$ is the Cartesian position vector, and ω is the circular frequency. The complex pressure P is assumed to satisfy the pressure-release boundary condition $P = 0$ at the ocean surface, the outgoing radiation condition at infinity, and the reduced wave equation

$$\rho\nabla\cdot[(1/\rho)\nabla P] + K^2 P = -4\pi\delta(\mathbf{x}-\mathbf{x}_0), \tag{1}$$

where the point $\mathbf{x}_0$ is the source location. The complex wavenumber $K = k + i\alpha\beta/k$ is used to account for sediment loss. The wavenumber is $k = \omega/c$, $\eta = (40\pi\log_{10} e)^{-1}$, β is the attenuation in decibels per wavelength (dB/λ), ρ is the density, and c is the sound speed.

We assume that variations in azimuth are negligible and solve Eq. (1) in cylindrical coordinates, with z being the depth below the ocean surface and r being the horizontal distance from a source at the depth z_0. Variations in range are assumed to be sufficiently weak so that $\partial\rho/\partial r$ can be ignored, which simplifies Eq. (1) to

$$\frac{\partial^2 P}{\partial z^2} - \frac{1}{\rho}\frac{\partial\rho}{\partial z}\frac{\partial P}{\partial z} + \frac{\partial^2 P}{\partial r^2} + \frac{1}{r}\frac{\partial P}{\partial r} + K^2 P = -(2/r)\delta(r)\delta(z-z_0). \tag{2}$$

We define $Q = \sqrt{r}P$, and for $r > 0$ Eq. (2) becomes

$$\frac{\partial^2 Q}{\partial z^2} - \frac{1}{\rho}\frac{\partial\rho}{\partial z}\frac{\partial Q}{\partial z} + \frac{\partial^2 Q}{\partial r^2} + \frac{Q}{4r^2} + K^2 Q = 0. \tag{3}$$

We assume that $r > r_0$, where $kr_0 \gg 1$, and drop the $O(r^{-2})$ term in Eq. (3) to obtain the farfield equation

$$\frac{\partial^2 Q}{\partial z^2} - \frac{1}{\rho}\frac{\partial\rho}{\partial z}\frac{\partial Q}{\partial z} + \frac{\partial^2 Q}{\partial r^2} + K^2 Q = 0. \tag{4}$$

For range-independent domains, Eq. (4) factors exactly to

$$\frac{\partial Q}{\partial r} = ik_0\sqrt{1 + \frac{K^2 - k_0^2 + L}{k_0^2}}\,Q, \tag{5}$$

where c_0 is a reference sound speed, $k_0 = \omega/c_0$, and

$$L = \frac{\partial^2}{\partial z^2} - \frac{1}{\rho}\frac{\partial\rho}{\partial z}\frac{\partial}{\partial z}. \tag{6}$$

Equation (5), which we refer to as PE$_{1,1}$, is an accurate approximation for many range-dependent problems in underwater acoustics and can be solved in terms of outgoing coupled modes.[13]

PE derivations are based on approximations of the function $\sqrt{1+x}-1$ for $|x| \lesssim 1$ such as the Taylor series

$$\sqrt{1+x} - 1 = \tfrac{1}{2}x - \tfrac{1}{8}x^2 + \tfrac{1}{16}x^3 - \cdots. \tag{7}$$

[a)] Present address: Naval Research Laboratory, Washington, DC 20375.

 0001-4966/89/091097-06$00.80

If $K \cong k_0$, the first term of this series and the approximation

$$(K^2 - k_0^2)/2k_0 \cong k - k_0 + i\eta\beta|k| \tag{8}$$

give the narrow-angle PE

$$\frac{\partial U}{\partial r} = i(k - k_0)U - \eta\beta|k|U + \frac{iL}{2k_0}U, \tag{9}$$

where $Q = U\exp(ik_0 r)$. The terms on the right side of Eq. (9) (from left to right) are: the refraction term, which accounts for variations in sound speed; the loss term, which accounts for sediment attenuation; and the diffraction term, which accounts for the vertical component of propagation.[10]

The first two terms of the Taylor series have been used to derive a wide-angle PE.[5] However, the higher-order PE's based on the Taylor series are relatively inefficient. Since the Taylor series diverges for $|x| > 1$, many terms in the series are required for problems involving large differences in sound speed or very-wide-angle propagation. Furthermore, higher-order PE's based on the Taylor series are difficult to implement because x is raised to powers, which results in operators raised to powers.

The wide-angle PE is based on a rational linear Padé approximation. A generalization of the wide-angle PE that is based on a ratio of polynomials[6] is difficult to implement because powers of x are involved. A generalization of the wide-angle PE that involves only first powers is based on the following Padé series[7]:

$$\sqrt{1+x} - 1 = \sum_{j=1}^{n} \frac{a_{j,n}x}{1 + b_{j,n}x} + O(x^{2n+1}), \tag{10}$$

where n is the number of terms in the Padé expansion and

$$a_{j,n} = [2/(2n+1)]\sin^2[j\pi/(2n+1)], \tag{11}$$

$$b_{j,n} = \cos^2[j\pi/(2n+1)]. \tag{12}$$

Since the Padé series is valid outside the radius of convergence of the Taylor series, relatively few terms are needed for $|x| \cong 1$. We illustrate this in Table I. The four-term Taylor series is better than the one-term Padé series for $x < 1$, but the one-term Padé series is better for $x > 1$. The two-term Padé series and the four-term Taylor series are both correct to $O(x^5)$ for small x. Yet the two-term Padé series is substantially better than the four-term Taylor series. The three-term Padé series is fairly accurate well beyond the radius of convergence of the Taylor series near $x = 3$.

TABLE I. Comparison of Taylor and Padé series.

x	Four-term Taylor	One-term Padé	Two-term Padé	Three-term Padé	$\sqrt{1+x} - 1$
0.25	0.118 01	0.117 65	0.118 03	0.118 03	0.118 03
0.50	0.224 12	0.222 22	0.224 72	0.224 74	0.224 74
0.75	0.318 70	0.315 79	0.322 74	0.322 87	0.322 88
1.00	0.398 44	0.400 00	0.413 79	0.414 20	0.414 21
1.25	0.456 39	0.476 19	0.499 04	0.499 96	0.500 00
1.50	0.481 93	0.545 45	0.579 31	0.581 05	0.581 14
1.75	0.460 78	0.608 70	0.655 23	0.658 12	0.658 31
2.00	0.375 00	0.720 00	0.795 84	0.802 21	0.802 78
2.50	0.080 57	0.769 23	0.861 24	0.869 94	0.870 83
2.75	−0.064 55	0.814 81	0.923 76	0.935 19	0.936 49
3.00	1.101 56	0.857 14	0.983 61	0.998 17	1.000 00

The Padé series gives the higher-order PE

$$\frac{\partial U}{\partial r} = ik_0 \sum_{j=1}^{n} \frac{a_{j,n}(L + K^2 - k_0^2)}{k_0^2 + b_{j,n}(L + K^2 - k_0^2)}U, \tag{13}$$

which we refer to as PE_n. Equation (13) can be solved with the method of alternating directions. This approach involves n steps with the jth step requiring the solution of the equation

$$[k_0^2 + b_{j,n}(L + K^2 - k_0^2)]\frac{\partial U}{\partial r} = ik_0 a_{j,n}(L + K^2 - k_0^2)U. \tag{14}$$

We solve Eq. (14) by first discretizing depth dependence with Galerkin's method as described in the Appendix. The resulting system is then solved with Crank–Nicolson integration.

A special version of PE_1 has been considered for application in shallow water.[12] Since sound-speed variations are very small in shallow water, a signal trapped in a shallow ocean is influenced more by diffraction than refraction. The shallow-water version of PE_1,

$$\frac{\partial U}{\partial r} = i(k - k_0)U - \eta\beta|k|U + \frac{2ik_0 L}{4k_0^2 + L}U, \tag{15}$$

is obtained from PE_1 by assuming that $|(K^2 - k_0^2)U| \ll |LU|$ in the water column. Equation (15) has the same refraction term as Eq. (9) but an improved diffraction term.

To illustrate the ability of PE_n to handle long-range and very-wide-angle propagation, we consider a waveguide 250 m thick with pressure-release top and bottom boundaries in which $c = 1500$ m/s. A 25-Hz point source is placed at $z = 25$ m, and we take $c_0 = 1500$ m/s. The eight normal modes for this problem propagate at approximately 7, 14, 21, 29, 37, 46, 57, and 74 deg from horizontal. The PE_n solutions (initialized with the normal-mode solution at $r = 0$) are compared with the normal-mode solution in Fig. 1. We observe that the PE_n solutions break down very rapidly with r for small n. However, the PE_6 solution is nearly perfect at $r = 4$ km.

We now consider a realistic example that illustrates an application of PE_n for low-frequency underwater acoustic propagation in deep water. In the water column, we assume the Munk sound-speed profile[14]

$$c(z) = c_{ch}\left\{1 + \mu\left[2\frac{z - z_{ch}}{H} + \exp\left(-2\frac{z - z_{ch}}{H}\right) - 1\right]\right\}, \tag{16}$$

where $\mu = 0.0071$, $c_{ch} = 1500$ m/s, $z_{ch} = 1000$ m, and $H = 1200$ m. The ocean depth is 5000 m. In the sediment, $c = 1850$ m/s, $\rho = 1.5$ g/cm^3, and $\beta = 0.5$ dB/λ. A 10-Hz point source is placed at $z = 200$ m, and we take $c_0 = 1500$ m/s. The homogeneous half-space field[15] is used to initialize the field at $r = 400$ m. The Lloyd's mirror beams produced by the source propagate at approximately 11, 34, and 70 deg. PE_1 should accurately account for the 11- and 34-deg beams for well beyond $r = 20$ km. From the PE_1 and PE_5 solutions appearing in Fig. 2, however, we observe that PE_1 cannot handle the 70-deg beam, which is partially reflected from the

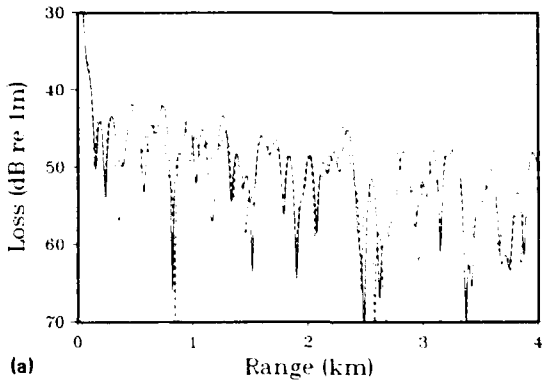

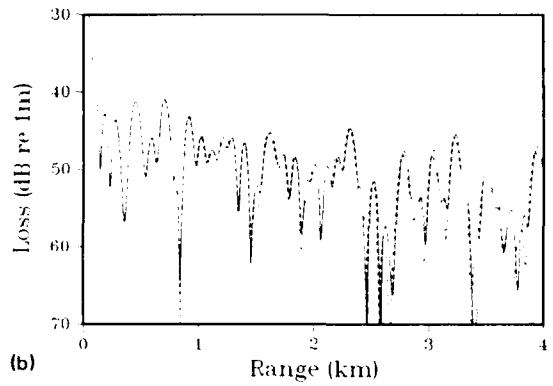

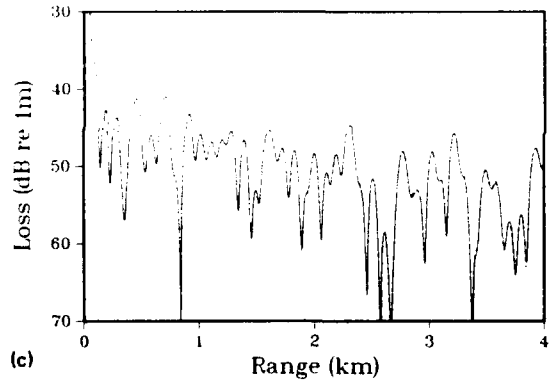

FIG. 1. Transmission loss at $z = 25$ m for a 25-Hz source in a waveguide with perfectly reflecting boundaries. The dashed curves are the normal mode solution. The solid curves are the PE_n solutions for (a) $n = 2$, (b) $n = 4$, and (c) $n = 6$.

ocean bottom and makes a significant contribution to the field for 5 km $< r <$ 15 km.

Since the parabolic approximation is based on an expansion about a reference wavenumber, it is not obvious that this approximation can be generalized to elastic media in which waves of different speeds exist. To investigate the possibility of generalizing PE_n to handle solid ocean bottoms, we consider a problem for which $c = 1500$ m/s in the water and the ocean depth is 200 m. In the fluid ocean bottom, $c = 1700$ m/s, $\rho = 1.5$ g/cm^3, and $\beta = 0.5$ dB/λ. A 50-Hz point source is placed at $z = 25$ m. The PE_2 solution for $c_0 = 1500$ m/s and the PE_{15} solution for $c_0 = 300$ m/s appear in Fig. 3. The agreement of the solutions suggests that a higher-order elastic PE based on the Padé series would handle both compressional and shear waves simultaneously.

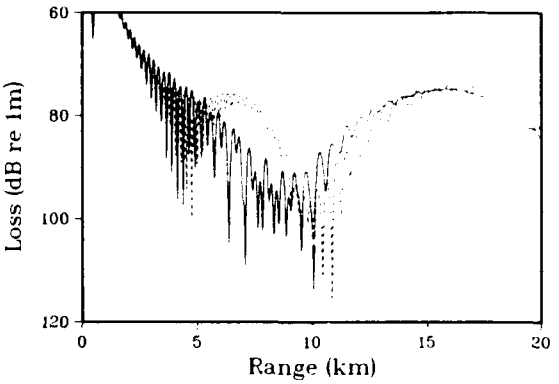

FIG. 2. Transmission loss at $z = 200$ m for a 10-Hz source in deep water. The dashed curve is the PE_1 solution. The solid curve is the PE_6 solution.

II. THE HIGHER-ORDER TDPE

Just as refraction is less important than diffraction for a signal trapped in shallow water, the effects of attenuation and dispersion are less important than refraction and diffraction for most problems. Thus we do not derive corrections for the attenuation/dispersion operator in the TDPE of Ref. 12. We assume that K is real (no attenuation) and that c is independent of ω (no dispersion) in the analysis and write Eq. (13) as

$$\frac{\partial U}{\partial r} = i\omega \sum_{j=1}^{n} \frac{\alpha_{j,n}\omega^2 + \beta_{j,n}L}{\gamma_{j,n}\omega^2 + \delta_{j,n}L} U, \tag{17}$$

where

$$\alpha_{j,n} = \frac{a_{j,n}}{c_0}\left(\frac{1}{c^2} - \frac{1}{c_0^2}\right), \tag{18}$$

$$\beta_{j,n} = \frac{a_{j,n}}{c_0}, \tag{19}$$

$$\gamma_{j,n} = \frac{1}{c_0^2} + b_{j,n}\left(\frac{1}{c^2} - \frac{1}{c_0^2}\right), \tag{20}$$

$$\delta_{j,n} = b_{j,n}. \tag{21}$$

To obtain a higher-order TDPE that is easy to solve numerically, we write Eq. (17) in the form

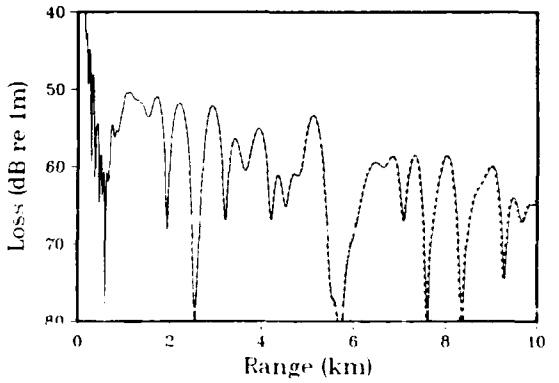

FIG. 3. Transmission loss at $z = 25$ m for a 50-Hz source in shallow water. The dashed curve is the PE_2 solution for $c_0 = 1500$ m/s. The solid curve is the PE_{15} solution for $c_0 = 300$ m/s.

$$\frac{\partial U}{\partial r} = i\omega \sum_{j=1}^{n} \left(\frac{\alpha_{j,n}}{\gamma_{j,n}} + \frac{(\beta_{j,n} - \alpha_{j,n}\delta_{j,n}/\gamma_{j,n})L}{\gamma_{j,n}\omega^2 + \delta_{j,n}L} \right) U. \quad (22)$$

We define

$$u(r,z,t) = \int_{-\infty}^{\infty} U(r,z,\omega)\exp(-i\omega t)\,d\omega \quad (23)$$

and invert the Fourier transform in Eq. (22) to obtain the higher-order TDPE:

$$\frac{\partial u}{\partial r} = -\sum_{j=1}^{n} \left(\frac{\alpha_{j,n}}{\gamma_{j,n}} + \frac{(\beta_{j,n} - \alpha_{j,n}\delta_{j,n}/\gamma_{j,n})L}{-\gamma_{j,n}(\partial^2/\partial t^2) + \delta_{j,n}L} \right) \frac{\partial u}{\partial t}, \quad (24)$$

which we refer to as TDPE_n.

The alternating directions solution of TDPE_n requires numerical solutions for each of the following $n+1$ equations:

$$\frac{\partial u}{\partial r} + \left(\sum_{j=1}^{n} \frac{\alpha_{j,n}}{\gamma_{j,n}} \right) \frac{\partial u}{\partial t} = 0, \quad (25)$$

$$\gamma_{j,n} \frac{\partial^3 u}{\partial r \partial t^2} - \delta_{j,n} L \frac{\partial u}{\partial r} = \left(\beta_{j,n} - \frac{\alpha_{j,n}\delta_{j,n}}{\gamma_{j,n}} \right) L \frac{\partial u}{\partial t}. \quad (26)$$

Since Eq. (25) is similar to the refraction term of the shallow-water TDPE, and Eq. (26) is similar to the diffraction term of the shallow-water TDPE, the numerical solutions developed in Ref. 12 can be modified slightly to obtain the time-domain solution of Eq. (22). In contrast, the time-domain solution of Eq. (17) requires the numerical solution of n equations similar to Eq. (26) as well as n third-order equations that are much more complicated than Eq. (25).

As in Ref. 12, the source function $f(t)$ is assumed to have compact support, and a time window $t_1 < t < t_2$ that contains the signal at all times is chosen. The boundary condition $u = 0$ is imposed at the pressure-release surface, deep within the sediment at $z = z_M$ from which no energy returns to the water column due to attenuation, and after the signal has passed the observer at $t = t_2$. The boundary conditions $u = \partial u/\partial t = 0$ are imposed before the signal is detected at $t = t_1$. Equation (25) is a first-order hyperbolic equation that can be solved with the Lax–Wendroff scheme.[16] Galerkin's method is used to discretize depth dependence in Eq. (26) as described in the Appendix. The resulting equation is then solved with Crank–Nicolson integration in r using centered differences in t while sweeping from $t = t_1$ to $t = t_2$.

To demonstrate the ability of TDPE_n to handle very-wide-angle propagation, we consider a waveguide of thickness 300 m with pressure-release top and bottom boundaries in which $c = 1500$ m/s. The Gaussian source $f(t) = \exp[-(\nu t)^2]$ is placed at $z = 25$ m, where $\nu = 150$ s^{-1}. The image solution, which is exact, is used to initialize the field at $r = 200$ m, and we take $c_0 = 1500$ m/s. The TDPE_1, TDPE_2, and TDPE_3 solutions are compared with the image solution in Fig. 4. Each of the solutions is very accurate for the first arrivals, which propagate at small angles. However, the agreement improves with n for the later arrivals, which propagate at larger angles.

In past studies of the TDPE, a stability condition for the numerical solution of the refraction operator has been discussed. However, the numerical solution of the diffraction operator appeared to be unconditionally stable based on numerical results. While performing the calculations for the previous example, however, we observed a new stability condition involving the grid spacings Δz and Δt. In a homogeneous medium, the numerical solution of the diffraction operator is unstable for $\Delta z = c_0 \Delta t$ and $n > 1$. The solution appears to be stable for all n if $\Delta z > A c_0 \Delta t$, where numerical experiments give $A \cong 1.4$.

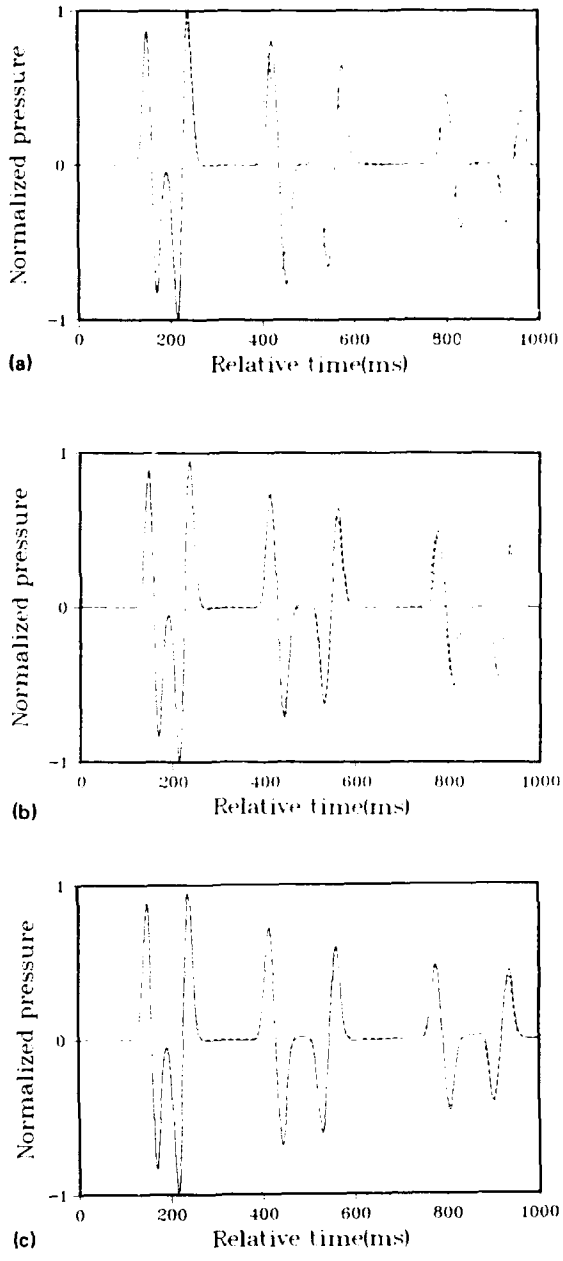

FIG. 4. Time series at $r = 500$ m and $z = 200$ m for a Gaussian pulse in a waveguide with perfectly reflecting boundaries. The dashed curves are the image solution. The solid curves are the (a) TDPE_1, (b) TDPE_2, and (c) TDPE_3 solutions.

To demonstrate the ability of TDPE_n to handle large variations in sound speed, we consider an ocean of depth 400 m in which c increases linearly from 1500 m/s at $z = 0$ to 1600 m/s at $z = 400$ m. In the sediment, $c = 1700$ m/s, $\rho = 1.5$ g/cm^3, and $\beta = 0.5$ dB/λ. The Gaussian source function with $\nu = 150$ s^{-1} is placed at $z = 50$ m, and we take

$c_0 = 1500$ m/s. The half-space field is used as an initial condition at $r = 100$ m. The plane-wave loss operator of Ref. 12 is used to model attenuation. However, we have found that greater accuracy is obtained by using c rather than c_0 in the loss operator. Sediment dispersion is neglected. The response to f is convolved as in Ref. 12 to obtain the response to a 50-Hz time-harmonic source. Transmission loss for the $TDPE_1$, PE_1, narrow-angle PE, and shallow-water PE_1 solutions appears in Fig. 5. The narrow-angle PE solution has large phase errors. The shallow-water PE_1 solution is better, but it too has a large error. The excellent agreement of the $TDPE_1$ and PE_1 solutions demonstrates the ability of $TDPE_1$ to accurately handle pulse propagation in deep water and shows that the plane-wave loss operator is accurate for this problem.

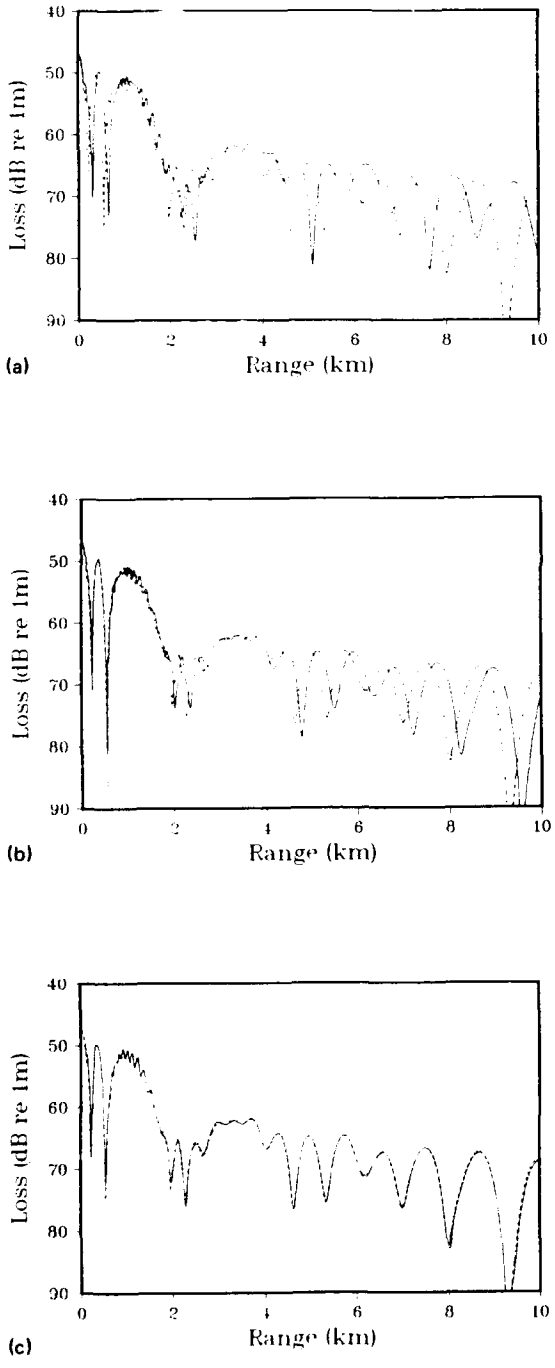

FIG. 5. Transmission loss at $z = 390$ m for a 50-Hz source in a refracting ocean. The dashed curves are the PE_1 solution. The solid curves are the (a) narrow-angle PE, (b) shallow-water PE_1, and (c) $TDPE_1$ solutions.

III. CONCLUSIONS

The phase error problem of the PE model has been completely eliminated. The higher-order PE based on a Padé series handles problems involving very-wide-angle propagation, propagation in the nearfield, propagation out to long range, and propagation in domains in which sound-speed variations are large. Numerical results suggest that the approach might be useful for elastic wave propagation for problems involving a superposition of compressional and shear waves. The higher-order PE was solved in the time domain, and a new stability condition was observed.

ACKNOWLEDGMENTS

This work has been approved for public release and was supported by the Office of Naval Research and the Naval Ocean Research and Development Activity (Contribution No. 221:021:89).

APPENDIX: DEPTH DISCRETIZATION WITH GALERKIN'S METHOD

Galerkin's method is effective for discretizing the relatively complicated depth operators in Eqs. (14) and (26), which have coefficient functions that may be discontinuous and involve derivatives. The depth grid points are defined as $z_i = i\Delta z$. The basis functions $\Psi_i(z)$ vanish for $|z - z_i| > \Delta z$, increase linearly from 0 to 1 over $z_{i-1} < z < z_i$, and decrease from 1 to 0 over $z_i < z < z_{i+1}$. We define $u_i(r,t) = u(r,z_i,t)$ as well as $\Theta_i = \Theta(z_i)$ and $\Phi_i = \Phi(z_i)$ for arbitrary functions Θ and Φ. The basis functions provide the approximations

$$u(r,z,t) \cong \sum_i u_i(r,t)\Psi_i(z), \tag{A1}$$

$$\Phi(z) \cong \sum_i \Phi_i \Psi_i(z), \tag{A2}$$

$$\Theta(z) \cong \sum_i \Theta_i \Psi_i(z). \tag{A3}$$

The following orthogonality condition is required to hold for all i:

$$\int \Psi_i(z) \left[\gamma_{j,n} \frac{\partial^2 u}{\partial r \partial t^2} - \delta_{j,n} L \frac{\partial u}{\partial r} - \left(\beta_{j,n} - \frac{\alpha_{j,n}\delta_{j,n}}{\gamma_{j,n}} \right) L \frac{\partial u}{\partial t} \right] dz = 0. \tag{A4}$$

Equation (26) is discretized by substituting Eq. (A1) for u and Eqs. (A2) and (A3) for the coefficient functions into Eq. (A4). The following approximations are obtained for the depth operators:

$$\Theta u\big|_{z=z_i} \cong \frac{\Theta_{i-1}+\Theta_i}{12}u_{i-1} + \frac{\Theta_{i-1}+6\Theta_i+\Theta_{i+1}}{12}u_i + \frac{\Theta_{i+1}+\Theta_i}{12}u_{i+1}, \tag{A5}$$

$$\Theta\frac{\partial^2 u}{\partial z^2}\bigg|_{z=z_i} \cong \frac{\Theta_i}{(\Delta z)^2}u_{i-1} - \frac{2\Theta_i}{(\Delta z)^2}u_i + \frac{\Theta_i}{(\Delta z)^2}u_{i+1}, \tag{A6}$$

$$\begin{aligned}\Phi\frac{\partial\Theta}{\partial z}\frac{\partial u}{\partial z}\bigg|_{z=z_i} \cong{}& \frac{(\Phi_{i-1}+2\Phi_i)(\Theta_{i-1}-\Theta_i)}{6(\Delta z)^2}u_{i-1} \\ &+ \frac{\Phi_{i-1}(\Theta_i-\Theta_{i-1})+2\Phi_i(2\Theta_i-\Theta_{i-1}-\Theta_{i+1})+\Phi_{i+1}(\Theta_i-\Theta_{i+1})}{6(\Delta z)^2}u_i \\ &+ \frac{(\Phi_{i-1}+2\Phi_i)(\Theta_{i+1}-\Theta_i)}{6(\Delta z)^2}u_{i+1}.\end{aligned} \tag{A7}$$

These approximations are also used to discretize depth in Eq. (14). As in Ref. 12, Θ corresponds to $\log(\rho)$ in Eq. (A7).

[1] F. D. Tappert, "The Parabolic Approximation Method," in *Wave Propagation and Underwater Acoustics*, edited by J. B. Keller and J. S. Papadakis (Springer, New York, 1977), Vol. 70, Lecture Notes in Physics.

[2] J. F. Claerbout, *Fundamentals of Geophysical Data Processing* (McGraw-Hill, New York, 1976), pp. 206–207.

[3] G. Botseas, D. Lee, and K. E. Gilbert, "IFD: Wide-Angle Capability," NUSC Tech. Rep. 6905 (1983).

[4] R. R. Greene, "The Rational Approximation to the Acoustic Wave Equation with Bottom Interaction," J. Acoust. Soc. Am. **76**, 1764–1773 (1984).

[5] D. F. St. Mary, D. Lee, and G. Botseas, "A Modified Wide Angle Wave Equation," J. Comput. Phys. **71**, 304–315 (1987).

[6] G. H. Knightly, D. Lee, and D. F. St. Mary, "A Higher-Order Parabolic Wave Equation," J. Acoust. Soc. Am. **82**, 580–587 (1987).

[7] A. Bamberger, B. Engquist, L. Halpern, and P. Joly, "Higher Order Paraxial Wave Equation Approximations in Heterogeneous Media," SIAM J. Appl. Math. **48**, 129–154 (1988).

[8] Reference 2, pp. 208–215.

[9] J. E. Murphy, "Finite-Difference Treatment of a Time-Domain Parabolic Equation: Theory," J. Acoust. Soc. Am. **77**, 1958–1960 (1985).

[10] B. E. McDonald and W. A. Kuperman, "Time Domain Formulation for Pulse Propagation Including Nonlinear Behavior at a Caustic," J. Acoust. Soc. Am. **81**, 1406–1417 (1987).

[11] M. D. Collins, "Low-Frequency, Bottom-Interacting Pulse Propagation in Range-Dependent Oceans," IEEE J. Ocean Eng. **13**, 222–228 (1988).

[12] M. D. Collins, "The Time-Domain Solution of the Wide-Angle Parabolic Equation Including the Effects of Sediment Dispersion," J. Acoust. Soc. Am. **84**, 2114–2125 (1988).

[13] R. B. Evans, "A Coupled Mode Solution for Acoustic Propagation in a Waveguide with Stepwise Depth Variations of a Penetrable Bottom," J. Acoust. Soc. Am. **74**, 188–195 (1983).

[14] W. H. Munk, "Sound Channel in an Exponentially Stratified Ocean with Applications to SOFAR," J. Acoust. Soc. Am. **55**, 220–226 (1974).

[15] M. D. Collins, "A Nearfield Asymptotic Analysis for Underwater Acoustics," J. Acoust. Soc. Am. **85**, 1107–1114 (1989).

[16] A. R. Mitchell and D. F. Griffiths, *The Finite Difference Method in Partial Differential Equations* (Wiley, New York, 1980), pp. 167–168.